Title

Environmental Stresses Increase Photosynthetic Disruption by Metal Oxide Nanomaterials in a Soil-Grown Plant.

Journal

ACS nano, 9(12)

ISSN

1936-0851

Authors

Conway, Jon R
Beaulieu, Arielle L
Beaulieu, Nicole L
et al.

Publication Date

2015-12-01

DOI

10.1021/acsnano.5b03091

Peer reviewed

Environmental Stresses Increase Photosynthetic Disruption by Metal Oxide Nanomaterials in a Soil-Grown Plant

Jon R. Conway,[†,‡] Arielle L. Beaulieu,[‡,§] Nicole L. Beaulieu,[‡,§] Susan J. Mazer,[∥] and Arturo A. Keller[*,†,‡]

[†]Bren School of Environmental Science & Management, University of California, Santa Barbara, California 93106-5131, United States, [‡]University of California Center for the Environmental Implications of Nanotechnology (UC CEIN), Los Angeles, California 90095-7227, United States, [§]Department of Environmental Studies, University of California, Santa Barbara, California 93106-5131, United States, and [∥]Department of Ecology, Evolution, and Marine Biology, University of California, Santa Barbara, California 93106-5131, United States

ABSTRACT Despite an increasing number of studies over the past decade examining the interactions between plants and engineered nanomaterials (ENMs), very few have investigated the influence of environmental conditions on ENM uptake and toxicity, particularly throughout the entire plant life cycle. In this study, soil-grown herbaceous annual plants (*Clarkia unguiculata*) were exposed to TiO_2, CeO_2, or $Cu(OH)_2$ ENMs at different concentrations under distinct light and nutrient levels for 8 weeks. Biweekly fluorescence and gas exchange measurements were recorded, and tissue samples from mature plants were analyzed for metal content. During peak growth, exposure to TiO_2 and CeO_2 decreased photosynthetic rate and CO_2 assimilation efficiency of plants grown under high light and nutrient conditions, possibly by disrupting energy transfer from photosystem II (PSII) to the Calvin cycle. Exposure $Cu(OH)_2$ particles also disrupted photosynthesis but only in plants grown under the most stressful conditions (high light, limited nutrient) likely by preventing the oxidation of a primary PSII reaction center. TiO_2 and CeO_2 followed similar uptake and distribution patterns with concentrations being highest in roots followed by leaves then stems, while $Cu(OH)_2$ was present at highest concentrations in leaves, likely as ionic Cu. ENM accumulation was highly dependent on both light and nutrient levels and a predictive regression model was developed from these data. These results show that abiotic conditions play an important role in mediating the uptake and physiological impacts of ENMs in terrestrial plants.

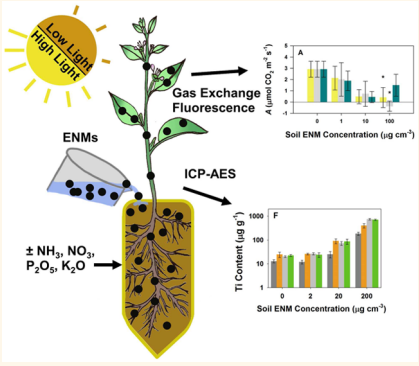

KEYWORDS: environmental stress · nanoparticle · uptake · phytotoxicity · photosynthesis · TiO_2 · CeO_2 · $Cu(OH)_2$

As the production and use of engineered nanomaterials (ENMs) grows each year, it becomes increasingly important to understand how these emerging pollutants are transported in the environment and to characterize their interactions with other organisms. Plants are the basis for many terrestrial food webs and are at risk of ENM exposure due to buildup in soils through biosolid fertilizer application, nanopesticide application, runoff, or atmospheric deposition.[1,2] Understanding how ENMs may affect plant performance, fruit and seed quality, and/or generate cascading effects on plant pollinators or herbivores is therefore essential to create informed policies regarding proper management of ENM use and disposal, in addition to the design of more environmentally benign ENMs.

A growing number of studies investigating the uptake and toxicity of ENMs in plants have been conducted in the past decade, and have generally found that both depend strongly on plant species and on the characteristics of the focal nanomaterials. For example, TiO_2 nanoparticles have been shown to have a toxic effect in vetch,[3] no effect in wheat seedlings,[4] and a positive effect on both photosynthetic rates[5] and chloroplast viability[6] in spinach, although it is unclear how much of this variability is due to the model species tested, the properties of the specific TiO_2 nanomaterials used, and the method of exposure (root *vs* foliar). Additionally, particle size has been shown

* Address correspondence to keller@bren.ucsb.edu.

Received for review May 21, 2015 and accepted October 27, 2015.

Published online 10.1021/acsnano.5b03091

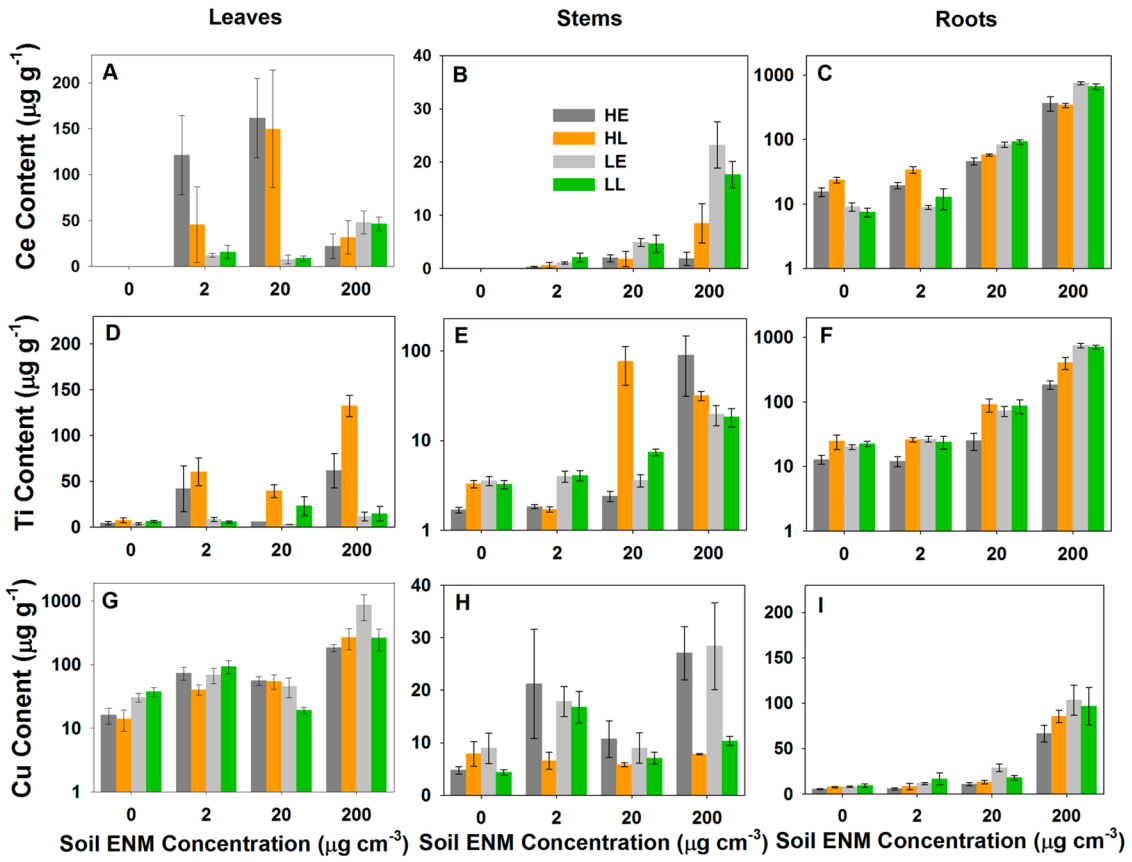

Figure 1. Tissue metal concentration of plants grown under high light excess nutrient (HE), high light limited nutrient (HL), low light excess nutrient (LE), and low light limited nutrient (LL) conditions. (A−C) Ce content of leaves, stems, and roots from CeO_2-exposed plants; (D−F) Ti content of leaves, stems, and roots from TiO_2-exposed plants; (G−I) Cu content of leaves, stems, and roots from $Cu(OH)_2$-exposed plants. Error bars are ±SE.

to have large impacts on ENM uptake and distribution patterns in plants, with smaller particles typically being taken up in higher amounts and distributed throughout the plant.[4,7−9] Smaller aggregate sizes achieved through surface coatings may be expected to show similar trends, but often the changes in surface charge and functionalization caused by these coatings are more important predictors of behavior than size alone.[10,11]

One aspect of plant/ENM interactions that has received little attention is the influence of abiotic environmental conditions on uptake and toxicity. These include factors such as water and nutrient availability, temperature, soil salinity and pH, and light intensity. Plant performance depends heavily on environmental conditions and may be more or less vulnerable to potential toxic effects under different growth scenarios. This has been shown for several non-nano pollutants. For example, high light intensities resulted in higher concentrations of As[12] and Cd[13] in sunflower and duckweed due to increased transpiration, and a range of unfavorable growing conditions have been found to increase damage from Fe-catalyzed reactive oxygen species (ROS) in many plant species.[14] Additionally, it was found in pea seedlings that nutrient stress (Fe depletion) increased the expression of transporter proteins that, in turn, increase cellular uptake of metals such as Cd.[15] In one of the few previous studies specifically investigating the interactions between abiotic growth conditions and ENM phytotoxicity, Josko and Oleszczuk[16] found that the toxicity of metal oxide ENMs to cress (*Lepidium sativum*) was enhanced under high light conditions and ameliorated at higher temperature. Building further understanding of how these factors affect the uptake and toxicity of ENMs in plants is key to accurate predictions of the overall impact of ENMs outside of the growth chamber or greenhouse and across both crop and wild species.

In this experiment, we investigated the uptake, translocation, and effects on growth and physiology of three metal oxide ENMs, CeO_2, TiO_2, and $Cu(OH)_2$, in soil-grown *Clarkia unguiculata* (Onagraceae) with different illumination and nutrient levels. *C. unguiculata* is an annual wildflower often used in ecological and genetic studies, and was selected here for its ease of growth, distinct tissues, and moderate lifespan (10−12 weeks) that would allow for subchronic effects to be detected. Additionally, we used individuals from wild populations with greater genetic variability[17] than crop plants typically used in nanotoxicological studies,[4,18,19]

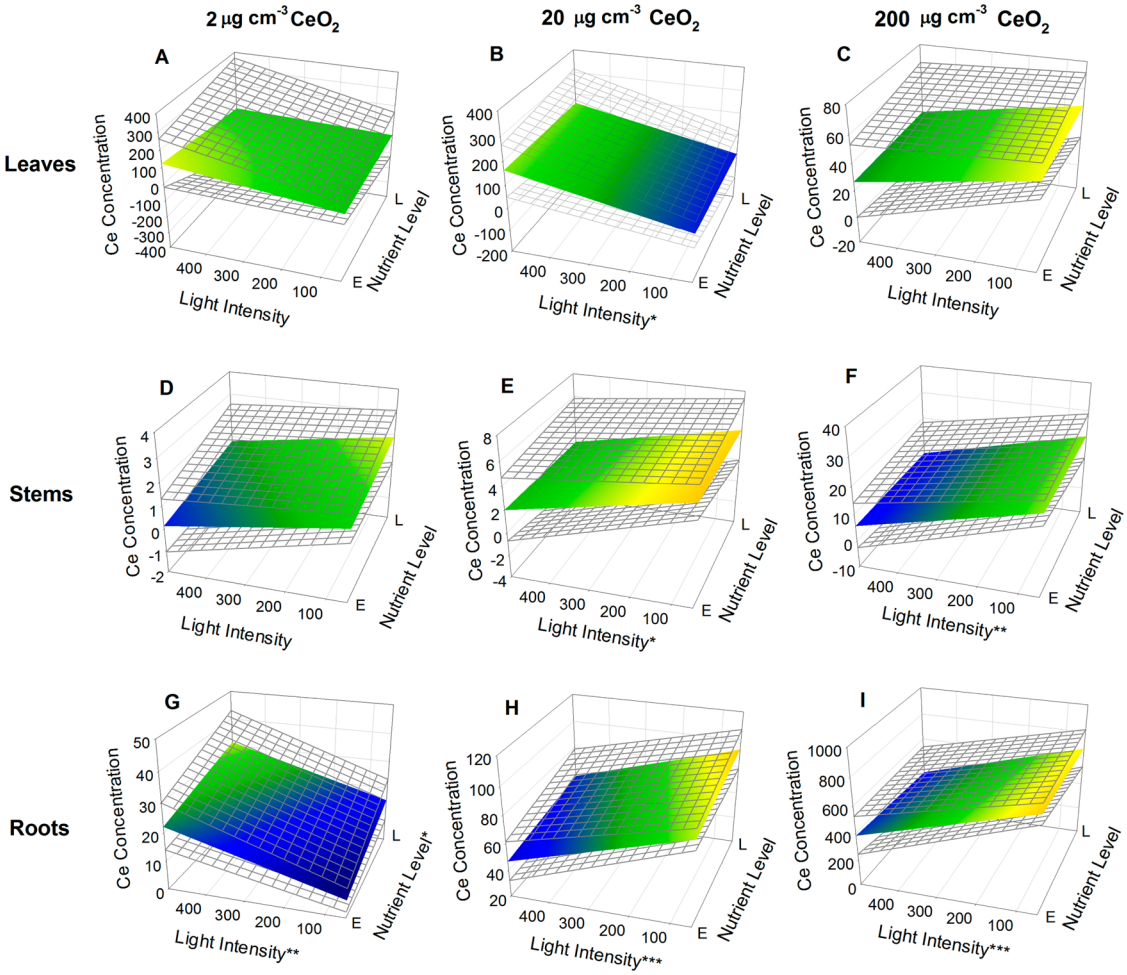

Figure 2. Predicted Ce concentrations (μg g^{-1}) in leaves, stems, and roots at 2, 20, and 200 μg cm^{-3} soil CeO_2 concentrations based on multiple regression results presented in Table S1. Cooler colors signify lower metal concentrations, while warmer colors signify higher metal concentrations. Transparent planes represent $\pm$1 SE. If Light Intensity (μmol_{photon} m^{-2} s^{-1}) or Nutrient Level (excess [E] or limited [L], defined in text) had a significant effect on tissue Ce Concentration, the corresponding axis label is marked with an asterisk. *$p < 0.05$, **$p < 0.01$, ***$p < 0.001$.

which makes this experiment conservative with respect to detecting the effects of ENM exposure on plant uptake and performance.

The ENMs we chose are widely used in nanoparticulate form in a number of commercial and industrial products and have release patterns that make them relevant for studies of terrestrial ecosystems.[20,21] Plant exposure levels were chosen to cover a range of ENM concentrations that we predicted to be environmentally relevant based on previous reports of exposure modeling and detection for CeO_2 and TiO_2. CeO_2 has been predicted to be present at levels up to about 1 mg/kg in roadside soils due to atmospheric deposition,[21] and while there are no direct measurements of soil TiO_2 concentrations of which we are aware, Kiser *et al.*[22] found TiO_2 in wastewater treatment plant (WWTP) solids at concentrations ranging from 1 to 6 mg kg^{-1}, which are spread on agricultural fields for fertilizer. The $Cu(OH)_2$ ENM used here is an agricultural biocide (Kocide 3000) and is recommended by the manufacturer for use at application rates of up to 18 g m^{-2} per season.[23] Overspray of this pesticide may have an impact on the surrounding vegetation.

We formulated several hypotheses to guide our investigation. First, we hypothesized that ENMs would be found in highest concentrations in the roots as the point of uptake, followed by leaves as the end point of transpiration, then stems as an intermediary between the two. Second, we also predicted that plants grown in high light would uptake and accumulate higher concentrations of ENMs in leaves due to higher rates of transpiration.[12] Third, we hypothesized that P would be positively correlated with ENM concentration in tissues due to sorption of phosphate from the soil. Natural metal oxides such as clays are known to strongly and preferentially sorb phosphate over other organic and inorganic ligands,[24] and research has shown that metal oxide ENMs can also sorb phosphorus and thereby potentially affect its bioavailability in soils and other environmental media.[25] Fourth, we hypothesized that higher light and lower nutrient conditions would be more physiologically stressful for

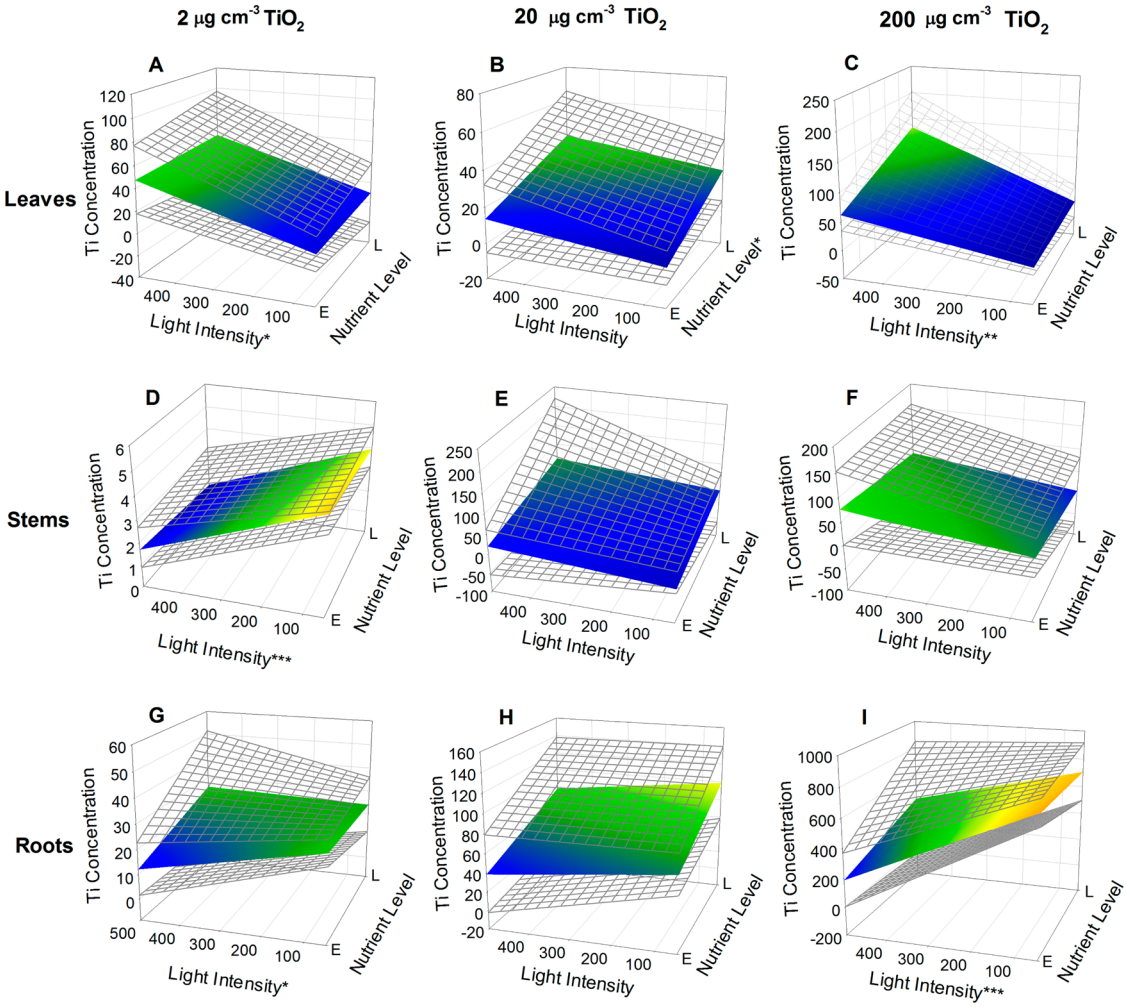

Figure 3. Predicted Ti concentrations (μg g^{-1}) in leaves, stems, and roots at 2, 20, and 200 μg cm^{-3} soil TiO_2 concentrations based on multiple regression results presented in Table S1. Cooler colors signify lower metal concentrations while warmer colors signify higher metal concentrations. Transparent planes represent $\pm$1 SE. If Light Intensity (μmol_{photon} m^{-2} s^{-1}) or Nutrient Level (excess [E] or limited [L], defined in text) had a significant effect on tissue Ti Concentration, the corresponding axis label is marked with an asterisk. *$p < 0.05$, **$p < 0.01$, ***$p < 0.001$.

Clarkia plants, and that highly stressed plants would be most vulnerable to ENM toxicity. Additionally, since TiO_2 and CeO_2 are photoactive and produce ROS when exposed to light,[26,27] we predicted that they would have the greatest effect in plants grown under high illumination by interfering with photosynthesis in leaves.

RESULTS AND DISCUSSION

ENM Uptake and Distribution. Metals from ENMs were taken up into all tissues in all treatments, although the amounts depended on ENM type, soil ENM concentrations, growth condition (high light excess nutrient (HE), high light limited nutrient (HL), low light excess nutrient (LE), and low light limited nutrient (LL)), and tissue type. Mean tissue metal concentrations can be seen in Figure 1, and results from multiple regressions can be seen in Figures 2–4 and Table S1. In general, Ce and Ti were found in highest concentration in roots (Figure 1C,F), while Cu was primarily found in leaves (Figure 1G), although relatively high concentrations of Ti were also seen in stems (Figure 1E). Background concentrations of Ti and Cu were found in all three tissues, while background Ce was only found in roots. Among plants in the Control group (those exposed to no supplemental nanoparticles), it is likely that Ce was not found in stems or leaves because it was not present in the soil at concentrations as high as Ti (Table 2), nor is it an essential micronutrient as is Cu.

Of the three ENMs to which plants were exposed, those exposed to CeO_2 and TiO_2 followed the pattern of distribution described in our first hypothesis, with concentrations being consistently highest in the roots followed by leaves then stems (Figure 1A–F). In $Cu(OH)_2$-exposed plants, however, Cu concentrations were roughly an order of magnitude higher in leaves than in roots (Figure 1G–I). Plants from all groups showed statistically significant positive correlations between exposure concentration and metal concentration in roots (multiple regressions in Table S1, $p < 0.05$)

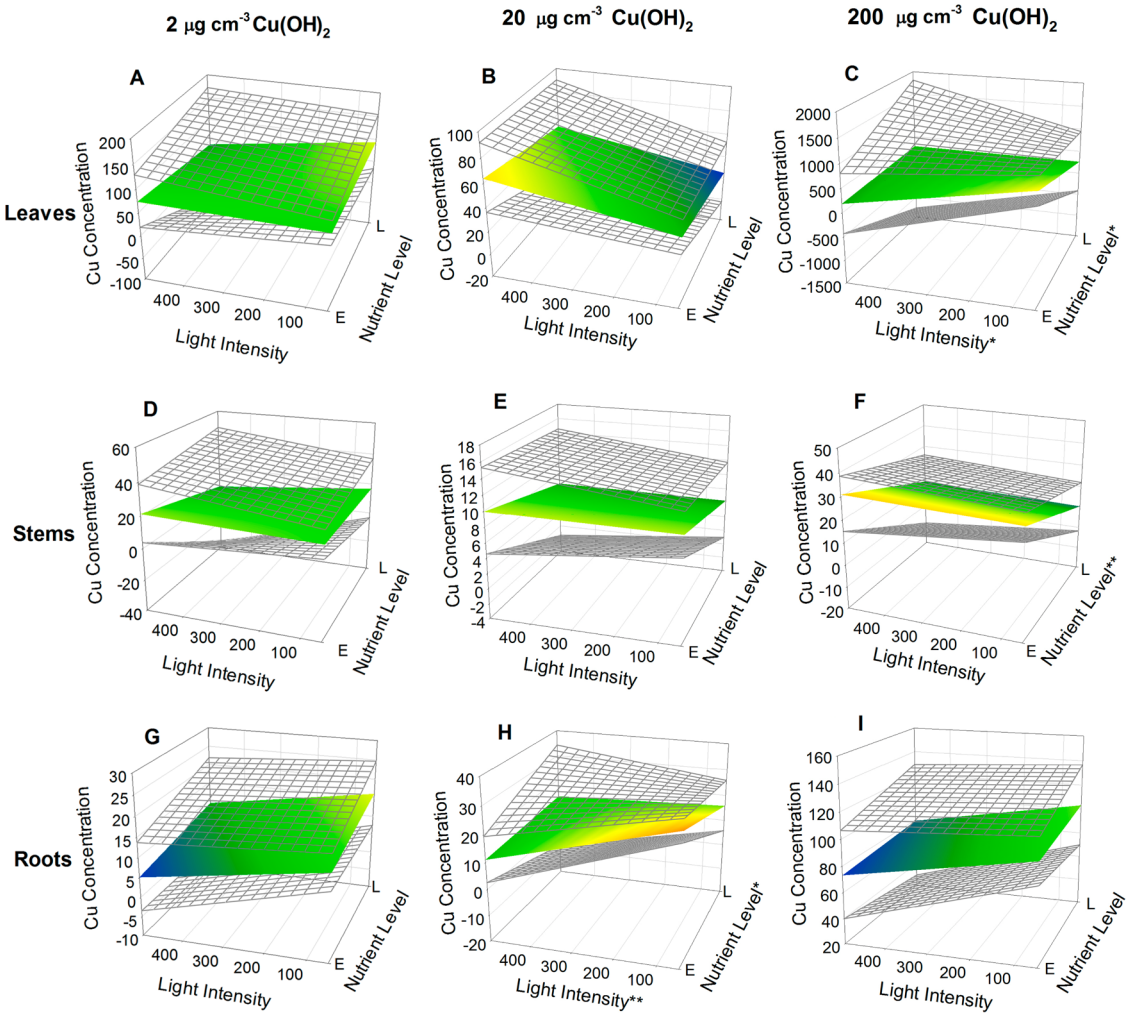

Figure 4. Predicted Cu concentrations (μg g^{-1}) in leaves, stems, and roots at 2, 20, and 200 μg cm^{-3} soil $Cu(OH)_2$ concentrations based on multiple regression results presented in Table S1. Cooler colors signify lower metal concentrations while warmer colors signify higher metal concentrations. Transparent planes represent ±1 SE. If Light Intensity (μmol_{photon} m^{-2} s^{-1}) or Nutrient Level (excess [E] or limited [L], defined in text) had a significant effect on tissue Cu Concentration, the corresponding axis label is marked with an asterisk. *$p < 0.05$, **$p < 0.01$.

and, with a few exceptions, tended to have the highest metal concentrations at the highest exposure level in all tissues. The most notable exceptions to this trend are the variable Ce and Ti content of leaves from plants grown under high light, excess nutrient (HE) and high light, limited nutrient conditions (HL) (Figure 1A,D). This reflects the high inter-leaf metal content variability for Ce and Ti and may be due to a randomized or patchy accumulation of these nanoparticles between leaves. There were no significant associations between leaf metal content and leaf node number, which is analogous to order of production (linear regressions, $p > 0.05$; data not shown). Since *C. unguiculata* leaves are produced in a temporal sequence along the height of the plant and are also larger lower on the plant, this indicates that ENM uptake into leaves was independent of both stage of growth and leaf size.

Growth conditions also played a role in ENM uptake, with plants grown under high light accumulating more Ce and Ti in their leaves than those grown in low light (Figures 2A and 3B, and Table S1, multiple regressions, $p < 0.001$) and HL leaves accumulating more Ti than HE (Figure 3A, Table S1, multiple regressions, $p < 0.01$). Along with the increased transpiration rates seen in plants grown under high light (discussed below), these findings validate our second hypothesis that high light plants would exhibit elevated uptake of ENMs to leaves due to increased transpiration. However, increased uptake of Cu into leaves and roots was found under low light conditions (Figure 4). These differences among ENM types in uptake and distribution are also likely to be due to differences in particle characteristics, particularly morphology and surface charge. The CeO_2 ENMs we used had a moderately high aspect ratio (Table 1) and thus had a smaller minimum dimension, which may allow them to pass through narrow vascular tissues in the stem more easily than the spherical TiO_2. Due to this physical size limitation, TiO_2 may also aggregate in the conductive tissues of the stems at higher concentrations, causing the buildup seen in Figure 1.

TABLE 1. ENM Physicochemical Properties

property	TiO_2	CeO_2	$Cu(OH)_2$
Primary particle diameter (nm)[a]	27 ± 4	rods: (67 ± 8) × (8 ± 1) polyhedra: 8 ± 1 nm	100−1000
Hydrodynamic diameter (nm)[b]	194 ± 7	231 ± 16	1532 ± 580
Target metal content (wt %)[c]	98.3	95.14	26.5 ± 0.9
Other elements present[d]	N.M.	N.M.	C, O, Na, Al, Si, S, Zn
Phase/structure	82% anatase, 18% rutile	Cubic ceria	Orthorhombic $Cu(OH)_2$
Morphology	Semispherical	Rods (≤10% polyhedra)	Spherical/polyhedra
Moisture content (wt %)	1.97	4.01	10.84
BET surface area ($m^2\ g^{-1}$)	51.5	93.8	15.71 ± 0.16
Isoelectric point	6.2	7.5	<3.0
Zeta potential (mV)[b]	+30.0 ± 2.2	+32.8 ± 1.0	−47.6 ± 4.3

[a] Dry powder measured with SEM/TEM. [b] Measured *via* dynamic light scattering (DLS) in nanopure water. [c] TiO_2 and CeO_2 purity measured with thermogravimetric analysis (TGA); $Cu(OH)_2$ purity was determined *via* ICP-AES. [d] Analysis done *via* XRD and EDS.

Particle charge likely plays a large role in determining distribution as well. Table S2 shows that all three ENMs used here had a weak negative charge in potting soil pore solution, although this was likely due to the high ionic strength and organic content of this soil shielding the particle surfaces and not a result of a direct alteration of the ENM crystal surface. Wang *et al.*[28] and Zhu *et al.*[29] found that under hydroponic conditions, well-dispersed particles coated with positively charged polymers (ζ-potential ≈ + 20 mV) are more readily taken up into plant roots compared to those coated with negatively charged polymers (ζ-potential ≈ −20 mV), which had higher accumulation in leaves. The results seen here provide confirmation of the importance of surface charge in ENM uptake and distribution in plants under more environmentally relevant conditions, *i.e.*, in soil and with polydisperse ENMs.

In addition to its surface charge, the tendency of $Cu(OH)_2$ to dissolve at low pH,[30,31] such as is found in the soil used in this study (Table 2), likely also contributes to its uptake behavior. Rhizosphere pH tends to be more acidic than the surrounding soil due to the release of protons by roots to stimulate and counterbalance the uptake of ions from the soil;[32] one effect of this acidity may be to dissolve a portion of the $Cu(OH)_2$. Dissolved Cu would, in turn, encounter less size exclusion than ENMs and be retained less in the roots and stems in addition to being actively transported to the leaves, consequently making Cu uptake and translocation less dependent on plant transpiration than CeO_2 or TiO_2. Although Cu is an essential component of several enzymes and other compounds in chloroplasts and mitochondria,[33] it can be toxic at higher concentrations.[34]

Last, although we predicted that P would be correlated with metal content in tissues due to physiochemical sorption of phosphate to the ENMs, it was only in root tissue of HL plants exposed to CeO_2 ENMs that we found a relationship. At root Ce concentrations below 100 $\mu g\ g^{-1}$, P was positively associated with Ce (linear regression, $R^2 = 0.870$, $p < 0.005$), but this trend

TABLE 2. Soil Properties

property	
Saturation percent (%)	514.5 ± 48.4
pH	5.74 ± 0.01
Electrical conductivity ($dS\ m^{-1}$)	2.55 ± 0.05
Cation exchange capacity (meq/100 g^{-1})	69.2 ± 1.2
Loss-on-ignition organic matter (%)	52.83 ± 0.91
Bulk density ($g\ cm^{-3}$)	0.086 ± 0.001
Exchangeable PO_4—P ($\mu g\ cm^{-3}$)	28.0 ± 0.2
Exchangeable NH_4—N ($\mu g\ cm^{-3}$)	0.884 ± 0.004
Exchangeable NO_3—N ($\mu g\ cm^{-3}$)	32.0 ± 0.8
Exchangeable K ($\mu g\ cm^{-3}$)	120. ± 0.
Total Ce ($\mu g\ cm^{-3}$)	0.599 ± 0.061
Total Cu ($\mu g\ cm^{-3}$)	0.100 ± 0.010
Total Ti ($\mu g\ cm^{-3}$)	1.38 ± 0.02

plateaued at higher concentrations. One possible explanation for this is that CeO_2 ENMs adsorbed P from the soil and were then sorbed into/onto the plant roots, but at higher exposure concentrations, the soil was depleted of readily available P for the ENMs to adsorb. Previous studies using hydroponic systems have shown increased P uptake in maize exposed to ZnO ENMs[35] and in spinach exposed to nZVI,[36] although these results were due to the uptake of dissolved metal/phosphate complexes rather than ENM-sorbed P. Rui *et al.*[37] observed the partial transformation of CeO_2 ENMs into particulate $CePO_4$ that were then taken up into hydroponically grown cucumber seedlings, although the general lack of correlation between tissue Ce and P concentrations suggests this process was not occurring to a significant extent in this study. Overall, our results did not indicate a significant relationship for *C. unguiculata* between ENM exposure and P bioavailability.

Physiological and Growth Impacts. We found that the physiological effects of ENM exposure on our test plants were strongly dependent on the environmental conditions under which plants were grown, namely, high light excess nutrient (HE), high light limited nutrient (HL), low light excess nutrient (LE), and low light limited nutrient (LL). By comparing photosynthetic

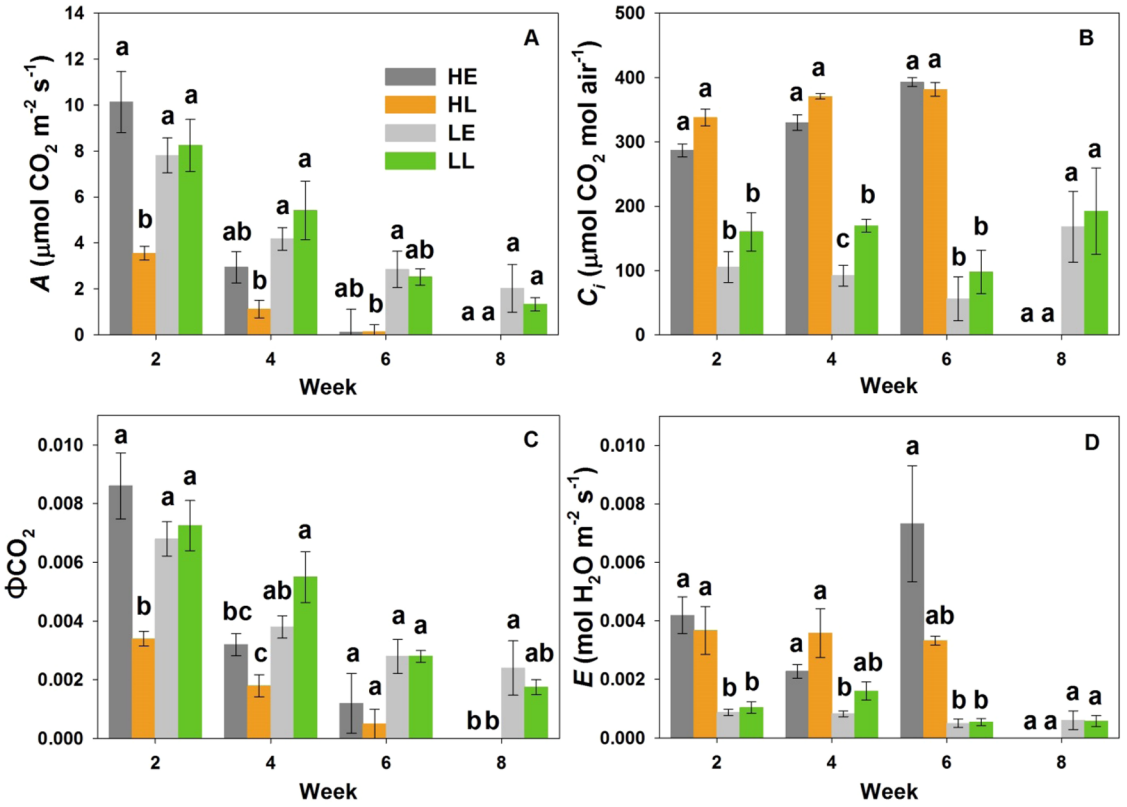

Figure 5. Physiological parameters of individuals not exposed to ENMs (zero concentration groups) grown under high light excess nutrient (HE), high light limited nutrient (HL), low light excess nutrient (LE), and low light limited nutrient (LL) conditions. (A) Photosynthetic rate (*A*); (B) intracellular CO_2 content (C_i); (C) quantum yield of CO_2 assimilation (ΦCO_2); (D) transpiration rate (*E*). Error bars are ±SE. HE = high light + excess nutrients, HL = high light + limited nutrients, LE = low light + excess nutrients, and LL = low light + limited nutrients. Within each week, mean values represented by distinct letters indicate significant differences detected by one-way ANOVA followed by posthoc Tukey's test or Kruskal−Wallis tests with multiple comparisons.

rates (*A*) and other physiological parameters of the zero concentration groups across growth conditions, we can establish baseline levels of stress[38] for each condition, which can be used to explain the trends seen in ENM-exposed plants. On the basis of the responses to growing conditions of *A*, transpiration rate (*E*), intracellular CO_2 (C_i), and quantum yield of CO_2 assimilation (ΦCO_2) in zero concentration groups (Figure 5), the relative rankings from most to least stressful growth condition appear to be HL > HE > LL ≈ LE. This ranking aligns with our hypothesis that higher light and lower nutrient conditions are the most stressful conditions imposed in this experiment.

For plants exposed to these ENMs, few significant correlations between the physiological parameters measured and ENM exposure concentration were seen at the second or sixth week of exposure, and by the eighth week, all high light plants had reached the end of their life cycle and ceased photosynthesizing. However, at the fourth week of exposure we found that in HE plants exposed to CeO_2 and TiO_2, *A* and ΦCO_2 decreased significantly and C_i increased significantly with increasing exposure concentration (linear regressions, $p < 0.05$, Figure 6, Table 3). This supports our final hypothesis and indicates that these two photoactive ENMs reduce photosynthetic rate by interfering with the assimilation of CO_2 required for photosynthesis, which results in a buildup of CO_2 within leaf cells. Additionally, there were no changes in ΦPSII in these plants, and this lack of correlation between ΦPSII and ΦCO_2 could indicate that energy transfer from photosystem II (PSII) to the Calvin cycle is being disrupted by the ENMs.[38]

This effect appears to be light-driven since no impacts of exposure concentration on any physiological parameters were seen in low light plants. High light conditions had the 2-fold impact of increasing particle uptake to leaves (Figure 1A,D) by increasing transpiration rates (Figure 5D) and possibly stimulating greater photoactivity of TiO_2 and CeO_2. The disruption of energy transfer observed may be due to the absorption of electrons from photosystem II (PSII) by the ENM upon the creation of an e^-/h^+ pair after excitation by a photon, or alternately through reactions with ROS produced by the ENM. Exposure to CeO_2 had slightly weaker effects on physiological parameters than TiO_2, and if the latter scenario is correct, this could be due to the lower relative ROS production rate of CeO_2 compared to TiO_2.[26] Barhoumi *et al.*[39] saw an inhibition of PSII and a corresponding increase in ROS in

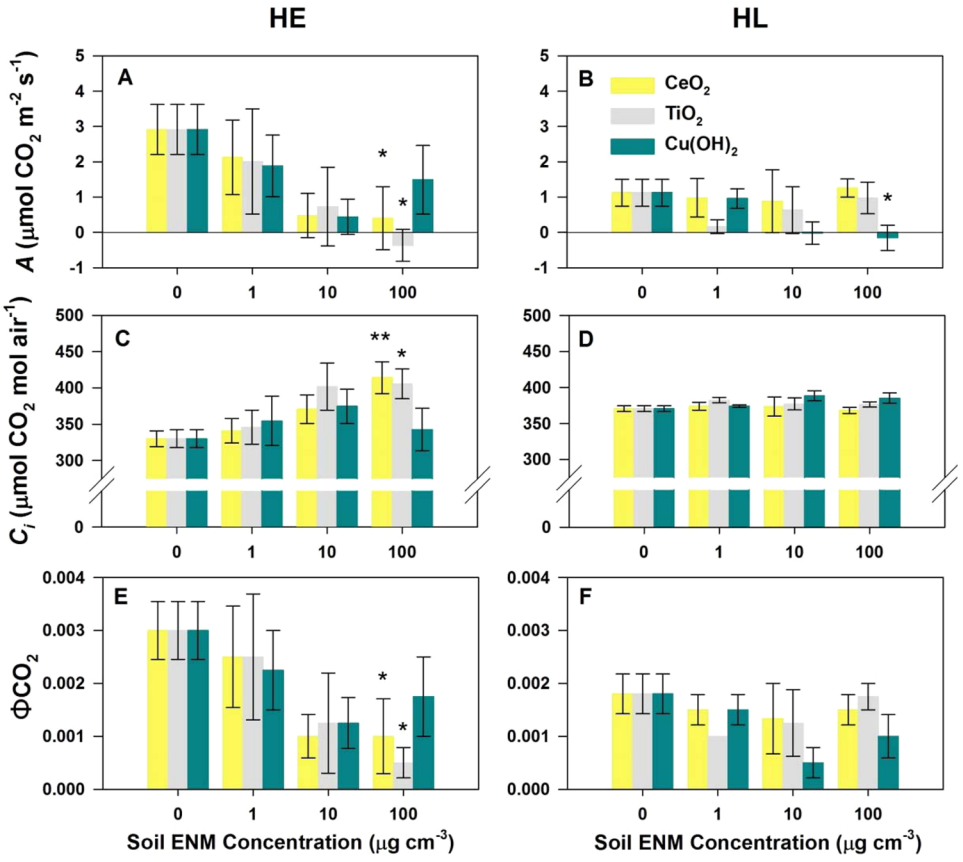

Figure 6. Physiological parameters of ENM-exposed groups during the fourth week of exposure. (A and B) Photosynthetic rate (A) of HE (A) and HL plants (B); (C and D) intracellular CO_2 content (C_i) of HE (C) and HL plants (D); (E and F) quantum yield of CO_2 assimilation (ΦCO_2) of HE (E) and HL plants (F). Error bars are ±SE. Treatments marked with asterisks at the highest concentrations are those that exhibit statistically significant correlation coefficients between soil ENM concentration and A, C_i, or ΦCO_2 based on linear regressions among individual plant values, as reported in Table 3. *$p < 0.05$, **$p < 0.01$.

TABLE 3. Slopes (±SE), R^2 Values, And Significance Levels from Linear Regressions among Individual Plants of Physiological Parameters (A, C_i, ΦCO_2, ΦPSII, and qL) on Soil ENM Concentrations during the Fourth Week of Exposure[a]

	HE			HL		
	CeO_2	TiO_2	$Cu(OH)_2$	CeO_2	TiO_2	$Cu(OH)_2$
A	−1.7 ± 0.8*	−1.6 ± 0.6*	−0.8 ± 0.8	0.1 ± 0.2	0.2 ± 0.4	−1.0 ± 0.3*
R^2	0.24	0.32	0.07	0.01	0.01	0.35
C_i	62 ± 17**	55 ± 22*	3.4 ± 20	−2.8 ± 5.6	1.0 ± 5.1	11 ± 5
R^2	0.47	0.30	0.00	0.02	0.00	0.20
ΦCO_2 ($\times 10^{-3}$)	−1.4 ± 0.7*	−1.8 ± 0.7*	0.7 ± 0.6	−0.2 ± 0.3	0.2 ± 0.4	−0.6 ± 0.4
R^2	0.24	0.29	0.09	0.01	0.02	0.13
ΦPSII ($\times 10^{-3}$)	−2.8 ± 7.9	−4.0 ± 7.6	−3.0 ± 7.8	−1.7 ± 3.8	−1.7 ± 3.2	12 ± 6
R^2	0.01	0.02	0.01	0.01	0.02	0.21
qL ($\times 10^{-2}$)	1.5 ± 2.5	3.3 ± 2.3	−1.1 ± 1.2	0.9 ± 1.4	−1.1 ± 1.0	3.5 ± 1.5*
R^2	0.02	0.12	0.05	0.026	0.08	0.25

[a] $N = 17$ for each treatment. Abbreviations are defined in text. *$p < 0.05$, **$p < 0.01$. Bivariate relationships in low light conditions are not shown because none were statistically significant.

Lemna gibba exposed to iron oxide ENMs, so similar phenomena may be occurring here. ROS production by TiO_2 and CeO_2 ENMs may also explain why no physiological effects were seen in HL plants, since plants upregulate antioxidant production at higher stress levels[40] that may counteract ROS produced by these ENMs.

Additionally, interference with photosynthetic mechanisms implies that CeO_2 and TiO_2 ENMs are able to penetrate or be actively transported not only into the leaf cells but also into the chloroplasts as well, and are able to intercalate themselves between thylakoid stacks to intercept electrons from PSII. Given that interthylakoid gaps can be on the order of 50−250 nm,[33]

individual particles or small aggregates would not necessarily be excluded based on size alone. Whiteside *et al.*[41] found uptake of NH_2-coated quantum dots <15 nm in diameter into bluegrass chloroplasts, so it is plausible that at least primary particles of TiO_2 and CeO_2 were able to enter the chloroplasts of our model plant. Both of these ENMs have limited dissolution and have been shown to be taken up into plant tissues as nanoparticles,[4,19,42] making it unlikely that any effects on photosynthesis are due to ionic Ti or Ce.

A similar decrease in *A* was seen in HL plants after 4 weeks of exposure to $Cu(OH)_2$, but without a corresponding change in ΦCO_2 or C_i (Figure 6). By further decreasing the already low photosynthetic rate of HL plants, $Cu(OH)_2$ had a larger relative impact than in HE, LE, or LL plants. This suggests that $Cu(OH)_2$ may affect photosynthesis through a different mechanism than TiO_2 and CeO_2. Additionally, we found that the fraction of oxidized PSII reaction centers (q_L) increased significantly with increasing exposure concentration (linear regression, $p < 0.05$, Table 3). In healthy plants, q_L is typically positively associated with photosynthetic production,[38] but since we found a negative correlation between $Cu(OH)_2$ exposure and photosynthesis (Table 3), the increases in q_L we observed were likely due to interference with the oxidation of the primary PSII quinine acceptor (Q_A) by light rather than increased photosynthetic efficiency.

Others have found similar oxidation of PSII reaction centers in plants exposed to ionic copper due to interference with the photon antennae of PSII,[43−45] which may indicate $Cu(OH)_2$ toxicity seen in this study is due to Cu ions released from the $Cu(OH)_2$ ENMs. In our system, $Cu(OH)_2$ could be dissolved either in the rhizosphere and taken up as ionic Cu or be taken up into the plant in particle form and dissolve within the plant tissues. However, since these $Cu(OH)_2$ particles has been shown to have increased dissolution at acidic pH and lower dissolution at basic pH,[31] the majority of dissolution probably occurs in the soil (pH 5.7) rather than in the neutral or slightly basic conditions of cell or chloroplast interiors.[46,47]

Linear growth rates (cm wk^{-1}), maximum height, leaf production rate, leaf loss rate (as leaves desiccate and senesce), maximum number of leaves, and week of maximum leaf production were calculated from physical measurements and are shown in Figures S1−S6. Few effects due to ENM exposure were seen under any growth condition, although LE plants exposed to $Cu(OH)_2$ had reduced growth rates, leaf production rates, and maximum number of leaves with increasing exposure concentrations (linear regressions, $p < 0.05$). Cu is an essential plant micronutrient but at high concentrations such as those observed in this experiment, Cu can decrease the uptake of other nutrients from the soil[48−50] and disrupt nitrogen metabolism.[43] Nutrient limitation caused by the presence of $Cu(OH)_2$ may have been responsible for limiting the growth of LE plants (Figures S1−S6). The lack of a growth response in HE plants exposed to CeO_2 and TiO_2 may be because, under high light conditions, reductions in CO_2 assimilation have been shown to have minimal impacts on C gain.[44]

CONCLUSIONS

The results presented here show the importance of two factors that have not received much attention when predicting the characteristics of plant/ENM interactions in environmentally relevant scenarios: the level of illumination and nutrient availability. On the basis of the effects of these factors on metal accumulation and gas exchange rates observed here, we can hypothesize plant populations that may be vulnerable to certain ENMs. Due to the high light and nutrient conditions of agricultural fields, we hypothesize that crop plants may be vulnerable to decreases in photosynthesis (and potentially yield) by photoactive ENMs such as TiO_2 and CeO_2, while plants growing in nutrient limited soils may be more vulnerable to nanoparticles with high dissolution rates such as $Cu(OH)_2$. However, since *C. unguiculata* uses the C_3 photosynthetic pathway (as do 85% of plant species),[51] the current study does not allow any predictions regarding how C_4 plants such as maize, sugarcane, or sorghum may be affected by ENM exposure. Since the C_4 pathway is more efficient in CO_2 assimilation and nutrient usage, C_4 plants may be able to compensate for reductions in photosynthesis caused by ENMs. Additionally, few to no effects of ENM exposure on plant performance were seen in the early or late stages of growth, when vertical growth and total carbon fixation (based on the number of leaves) were low. This suggests that these plants are most vulnerable to photosynthesis disruption by ENMs during the period of highest metabolic activity (*i.e.*, at later growth stages).

Although uptake of ENMs by soil grown plants has been reported before,[16,19,52−54] we demonstrate that stress factors correlate with metal accumulation. Since plants are typically at the base of food webs, this trend has important implications for the possibility of cascading effects through trophic transfer. A limited number of studies have measured trophic transfer in terrestrial systems, but Hawthorne, Roche, Xing, Newman, Ma, Majumdar, Gardea-Torresdey and White[7] recently observed transfer of CeO_2 ENMs in a terrestrial food chain from primary producer (zucchini) to primary consumer (cricket) to secondary consumer (spider), finding that ENMs were accumulated and transferred at higher concentrations than either bulk CeO_2 or ionic Ce. Judy *et al.*[55] also found significant biomagnification of Au ENMs in hornworms that were fed tobacco leaves. However, we found that TiO_2 and CeO_2 were highly concentrated in root tissue, which may result in high dietary exposure concentrations for root herbivores. This accumulation of ENMs in root tissue may also mean that decomposing plant roots could act as a

hotspot for ENM release into the soil, impacting local fungal, microbial and animal communities. On the other hand, this provides insight into possible future phytoremediation of sites contaminated with specific types of ENMs.

On the basis of the observations reported here, we recommend that future studies continue to investigate the influence of environmental conditions on plant/ENM interactions throughout the life cycle of individual plants. Additionally, these results highlight the applicability of detailed fluorescence and gas exchange measurements in determining a mechanistic understanding of the impacts of ENM exposure on plant physiology.

METHODS

Nanoparticle Characterization and Preparation. Three nanomaterials were used in these experiments: TiO_2, CeO_2, and $Cu(OH)_2$. TiO_2 and CeO_2 nanomaterials used in this experiment are fully characterized in Keller *et al.*[56] and $Cu(OH)_2$ is characterized in Adeleye, Conway, Perez, Rutten and Keller.[31] A summary of relevant properties can be found in Table 1. TiO_2 and CeO_2 ENMs were provided by Evonik Degussa Corp. (U.S.) and Meliorum Technologies (U.S.), respectively. $Cu(OH)_2$ particles were purchased from DuPont as the commercially available agricultural biocide Kocide 3000. TiO_2 particles were semispherical with a primary particle size of 27 ± 4 nm with a crystalline structure of 82% anatase and 18% rutile. Particle size after 30 min of sonication in deionized water (DI) was 194 ± 7 nm. CeO_2 particles were primarily rods with dimensions of $(67 \pm 8) \times (8 \pm 1)$ nm with $\leq$10% as polyhedra of diameter 8 ± 1 nm. Crystal structure was ceria cubic and particle size in DI after sonication for 30 min was 231 ± 16 nm. Kocide 3000 is composed of spherical composites on the order of 50 μm made up of irregular nano- to microscale $Cu(OH)_2$ embedded in a carbon-based matrix that rapidly dissolves in water to release polydisperse $Cu(OH)_2$ particles approximately 1500 ± 600 nm in diameter. Once the carbon matrix dissolves, it is likely the $Cu(OH)_2$ particles have a minimal barrier for aggregation, resulting in the strong aggregation seen in Table 1. ENM stock suspensions were prepared for each application as 1 g L^{-1} and bath sonicated for 30 min. Dilutions were not resonicated.

Plant Exposure and Growth Conditions. *C. unguiculata* is an annual hermaphroditic flowering shrub native to oak/pine woodlands and disturbed slopes in central California. Additional details can be found in Dudley *et al.*[57] and Vasek.[17] Seeds were collected from a field site in Kern County, CA (35° 41.453′ N, 118° 43.911′ W, elev. 2830 ft) in July 2008 and stored with desiccant in darkness at 4 °C until use. Seeds were randomly sampled from 10 maternal families, plated on agar in covered Petri dishes (8 g L^{-1}), vernalized in darkness for 5 days at 4 °C, and then germinated under ambient light at room temperature for an additional 5 days. Seedlings were then transplanted into 2.5 cm diameter × 16.34 cm long cylindrical plastic growing tubes (Ray Leach Cone-tainers; Stuewe and Sons, Tangent, OR) (one seedling per tube) containing 17 ± 0.1 g of a 1:20 mixture of worm castings to a peat moss/perlite/dolomitic limestone potting soil (Sunshine Mix #4, Sun Gro Horticulture). Soil properties other than Ce, Ti, and Cu content were measured at the UC Davis Analytical Lab (http://anlab.ucdavis.edu/) and are shown in Table 2. After transplantation, seedlings were kept moist and allowed to grow for 2.5 weeks before ENM exposure to allow them to become established, after which they were grown for an additional 8 weeks until they had completed their life cycle. Plants were grown in growth chambers under a 14:10 h 21:13 °C day/night cycle and exposed to variable light levels (detailed below).

Plants were grown under a total of four different environmental conditions: high light + excess nutrients (HE), high light + limited nutrients (HL), low light + excess nutrients (LE), and low light + limited nutrients (LL). Plants were grown under photosynthetic photon flux densities (PPFD) of 500 (high) or 50 (low) $\mu mol_{photon}\ m^{-2}\ s^{-1}$. These light conditions are roughly analogous to those on a partly cloudy day or a shaded understory. Excess nutrient conditions were achieved through the addition of 140 ± 3 mg fertilizer pellets (19-6-12 Osmocote Smart Release Indoor & Outdoor Plant Food) prior to seedling transplantation, corresponding to 70.7 ± 1.5 μg NH_3 per cm^3 soil, 63.6 ± 1.5 $\mu g\ cm^{-3}$ NO_3, 42.4 ± 1.0 $\mu g\ cm^{-3}$ P_2O_5, and 84.8 ± 2.0 $\mu g\ cm^{-3}$ K_2O released over the course of the experiment. Plants grown with limited nutrients did not receive fertilizer. Four replicates were grown per ENM, concentration, light condition, and nutrient level, and five control replicates were grown per light condition and nutrient level that were not exposed to ENMs for a total of 164 individuals.

Starting in the second week of growth, 50 mL of 0, 1, 10, or 100 mg L^{-1} TiO_2, CeO_2, or $Cu(OH)_2$ suspensions were slowly poured onto the soil surface of each individual container to allow for absorption into the soil. This was repeated weekly for a total of 8 weeks to result in a soil contamination rate of 0, 0.25, 2.5, or 25 μg ENM per cm^3 soil per week, or 0, 2.9, 29, or 290 mg kg^{-1} wk^{-1}. Plant heights and total leaf counts were recorded each week starting at the second week after seedling transplantation and physiological measurements were made every other week from the second week following the initiation of ENM exposure.

Physiological Measurements. Physiological measurements follow methods outlined in Dudley *et al.*[58] Photosynthetic assimilation rate ($\mu mol_{CO2}\ m^{-2}_{leaf\ area}\ s^{-1}$, A), transpiration rate ($mol_{H2O}\ m^{-2}_{leaf\ area}\ s^{-1}$, E), photosystem II quantum yield efficiency (ΦPSII), quantum yield of CO_2 assimilation ($\mu mol_{CO2}\ \mu mol^{-1}_{photon}$, ΦCO_2), photochemical quenching (q_P), electron transport rate ($\mu mol_{photon}\ m^{-2}_{leaf\ area}\ s^{-1}$, ETR), intercellular CO_2 concentration ($\mu mol_{CO2}\ mol^{-1}_{air}$, C_i), and various fluorescence parameters (F_o' and F_s) were measured from light-adapted leaves using a portable IR gas exchange analyzer (IRGA, LiCor 6400; Licor, Lincoln, NE) with a LiCor 6400-40 fluorometer light source. The fraction of oxidized PSII reaction centers (q_L) were calculated from eq 1.[59]

$$q_L = q_P \cdot \frac{F_o'}{F_S} \quad (1)$$

Leaves were measured on plants sampled in random order between 0800 and 1200 h using the following settings: PARi = 1500 ± 2, stomatal ratio = 0.5, flow = 500 $\mu mol\ mol^{-1}$, and reference CO_2 chamber concentration = 400 $\mu mol_{CO2}\ mol^{-1}$. Parameters were measured when photosynthetic, conductance, and fluorescence rates were stable (photo: slope < 1 for 10 s; conductance: slope < 0.05 for 10 s; fluorescence: dn/dt slope < 50 for 10 s). Leaf node position on the stem relative to the cotyledons was recorded for each measurement. If sampled leaves were not large enough to fill the 2 cm^{-2} IRGA chamber, the surface of the gasket that seals the chamber (when closed) was covered with ink, thereby stamping an image of the chamber's boundary on the leaf surface. A photograph of the leaf was taken and analyzed using ImageJ (National Institute of Health, Bethesda, MD; available at http://rsbweb.nih.gov/ij) to determine the leaf area that was exposed within the chamber, which was then used to recompute physiological parameters.

Elemental Detection. Plants were sacrificed and leaf, stem, and root samples were collected after 8 weeks of ENM exposure. Several leaves were collected at different heights and 5–6 cm segments of stem were taken from the middle of each plant and analyzed separately. Roots were thoroughly cleaned of any visible soil particles and were serially rinsed in clean baths of deionized water and 2% HNO_3 before analysis to facilitate removal of adsorbed ENMs on the root surfaces. Plant and soil metal characterization samples were vacuum-dried at 60 °C for 3 days, weighed, and digested in *aqua regia* (1:3 HNO_3/HCl) in a

microwave digestion system (Multiwave Eco, Anton Paar) at 200 °C for 1.5 h. Samples were then analyzed for Ti, Ce, Cu, and P *via* inductively coupled plasma atomic emission spectroscopy (ICP-AES, iCAP 6300 Thermo Scientific, Waltham, MA). Detection limits for all elements tested were approximately 5 μg L^{-1}. Standard solutions and blanks were measured every 15−20 samples for quality assurance.

Tissue metal concentrations for all three ENMs are reported as ionic, although neither CeO_2 nor TiO_2 was expected to dissolve to a significant degree under the conditions used in this experiment. TiO_2 is known to be highly insoluble in water and CeO_2 is similarly insoluble at pHs similar to those found in the potting soil used here (5.7).[60] Additionally, both ENMs have been found to be taken up into a variety of plant species in nanoparticulate form.[4,42,52,61] However, the $Cu(OH)_2$ ENM used here is known to undergo partial dissolution under acidic conditions[30,31] and will likely be at least partially present either as ionic Cu^{1+}/Cu^{2+} or as part of a complex with ions from the surrounding media.

Statistical Analysis. For each ENM, multiple regressions were used to model the effects of Soil ENM Concentration, Light Level, Nutrient Level, Tissue Type, and the interactions between these variables on Tissue Metal Concentrations. One-way linear regressions were used to determine the effects of Soil ENM Concentration or ENM Addition Rate on physiological (A, C_i, ΦCO_2, $\Phi PSII$, and q_L) and physical growth parameters (linear growth rates [cm wk^{-1}], maximum height, leaf production rate, leaf loss rate [as leaves desiccate and senesce], maximum number of leaves, and week of maximum leaf production). Separate regressions were performed for each growth condition, and Soil ENM Concentrations or ENM Addition Rates were $\log(x + 1)$ transformed to improve correlations with physiological and physical growth parameters. To determine the dependence of plant physiological rates on environmental conditions in the absence of ENM exposure, one-way ANOVA with posthoc Tukey's HSD tests or Kruskal−Wallis tests with multiple comparisons were used to detect the effects of growing conditions on photosynthetic rate (A), intracellular CO_2 (C_i), quantum yield of CO_2 assimilation (ΦCO_2), and transpiration rate (E) among plants that were not exposed to ENMs. Levene's tests were used to ensure homogeneity of variance and if data were not homogeneously distributed nonparametric tests were used. Statistical analyses were performed using Microsoft Excel 2007 and the statistical software R (v. 2.11.1).

Conflict of Interest: The authors declare no competing financial interest.

Supporting Information Available: The Supporting Information is available free of charge on the ACS Publications website at DOI: 10.1021/acsnano.5b03091.

Six additional figures showing maximum height, leaf production rate, leaf loss rate, maximum number of leaves, and week of maximum leaf production for all treatments and one additional table showing results from multiple regressions of tissue metal concentrations (PDF)

Acknowledgment. This work was supported in part by the National Science Foundation and the U.S. Environmental Protection Agency under Cooperative Agreement No. NSF-EF0830117, and by National Science Foundation Grant EF-0742521. Any opinions, findings, and conclusions or recommendation expressed in this material are those of the authors and do not necessarily reflect the views of the National Science Foundation or the U.S. Environmental Protection Agency. The authors would like to thank A. Strom at the UCSB MRL for her help with the ICP-AES. The MRL Shared Experimental Facilities are supported by the MRSEC Program of the NSF under Award No. DMR 1121053; a member of the NSF-funded Materials Research Facilities Network.

REFERENCES AND NOTES

1. Gottschalk, F.; Nowack, B. The Release of Engineered Nanomaterials to the Environment. *J. Environ. Monit.* **2011**, *13*, 1145–1155.
2. Keller, A. A.; Lazareva, A. Predicted Releases of Engineered Nanomaterials: From Global to Regional to Local. *Environ. Sci. Technol. Lett.* **2014**, *1*, 65–70.
3. Ruffini Castiglione, M.; Giorgetti, L.; Cremonini, R.; Bottega, S.; Spano, C. Impact of TiO2 Nanoparticles on *Vicia Narbonensis L.*: Potential Toxicity Effects. *Protoplasma* **2014**, *251*, 1471–1479.
4. Larue, C.; Laurette, J.; Herlin-Boime, N.; Khodja, H.; Fayard, B.; Flank, A. M.; Brisset, F.; Carriere, M. Accumulation, Translocation and Impact of TiO2 Nanoparticles in Wheat (*Triticum Aestivum* Spp.): Influence of Diameter and Crystal Phase. *Sci. Total Environ.* **2012**, *431*, 197–208.
5. Gao, F.; Liu, C.; Qu, C.; Zheng, L.; Yang, F.; Su, M.; Hong, F. Was Improvement of Spinach Growth by Nano-TiO2 Treatment Related to the Changes of Rubisco Activase? *BioMetals* **2008**, *21*, 211–217.
6. Hong, F. H.; Yang, F.; Liu, C.; Gao, Q.; Wan, Z. G.; Gu, F. G.; Wu, C.; Ma, Z. N.; Zhou, J.; Yang, P. Influences of Nano-TiO2 on the Chloroplast Aging of Spinach under Light. *Biol. Trace Elem. Res.* **2005**, *104*, 249–260.
7. Hawthorne, J.; Roche, R. D.; Xing, B. S.; Newman, L. A.; Ma, X. M.; Majumdar, S.; Gardea-Torresdey, J.; White, J. C. Particle-Size Dependent Accumulation and Trophic Transfer of Cerium Oxide through a Terrestrial Food Chain. *Environ. Sci. Technol.* **2014**, *48*, 13102–13109.
8. Gui, X.; He, X.; Ma, Y. H.; Zhang, P.; Li, Y. Y.; Ding, Y. Y.; Yang, K.; Li, H. F.; Rui, Y. K.; Chai, Z. F.; et al. Quantifying the Distribution of Ceria Nanoparticles in Cucumber Roots: The Influence of Labeling. *RSC Adv.* **2015**, *5*, 4554–4560.
9. Zhang, W.; Ebbs, S. D.; Musante, C.; White, J. C.; Gao, C.; Ma, X. Uptake and Accumulation of Bulk and Nanosized Cerium Oxide Particles and Ionic Cerium by Radish (*Raphanus Sativus L.*). *J. Agric. Food Chem.* **2015**, *63*, 382–390.
10. Parsons, J. G.; Lopez, M. L.; Gonzalez, C. M.; Peralta-Videa, J. R.; Gardea-Torresdey, J. L. Toxicity and Biotransformation of Unocated and Coated Nickel Hydroxide Nanoparticles on Mesquite Plants. *Environ. Toxicol. Chem.* **2010**, *29*, 1146–1154.
11. Schwabe, F.; Schulin, R.; Limbach, L. K.; Stark, W.; Buerge, D.; Nowack, B. Influence of Two Types of Organic Matter on Interaction of CeO2 Nanoparticles with Plants in Hydroponic Culture. *Chemosphere* **2013**, *91*, 512–520.
12. Yadav, G.; Srivastava, P. K.; Singh, V. P.; Prasad, S. M. Light Intensity Alters the Extent of Arsenic Toxicity in *Helianthus Annuus L.* Seedlings. *Biol. Trace Elem. Res.* **2014**, *158*, 410–421.
13. Gaur, J. P.; Noraho, N. Role of Certain Environmental Factors on Cadmium Uptake and Toxicity in *Spirodela Polyrhiza* (L.) Schleid. And *Azolla Pinnata* R.Br. *Biomed. Environ. Sci.* **1995**, *8*, 202–210.
14. Becana, M.; Moran, J. F.; Iturbe-Ormaetxe, I. Iron-Dependent Oxygen Free Radical Generation in Plants Subjected to Environmental Stress: Toxicity and Antioxidant Protection. *Plant Soil* **1998**, *201*, 137–147.
15. Cohen, C. K.; Fox, T. C.; Garvin, D. F.; Kochian, L. V. The Role of Iron-Deficiency Stress Responses in Stimulating Heavy-Metal Transport in Plants. *Plant Physiol.* **1998**, *116*, 1063–1072.
16. Josko, I.; Oleszczuk, P. Influence of Soil Type and Environmental Conditions on ZnO, TiO2 and Ni Nanoparticles Phytotoxicity. *Chemosphere* **2013**, *92*, 91–99.
17. Vasek, F. C. Outcrossing in Natural Populations 0.2. *Evolution* **1965**, *19*, 152–156.
18. Wang, Z. Y.; Xie, X. Y.; Zhao, J.; Liu, X. Y.; Feng, W. Q.; White, J. C.; Xing, B. S. Xylem- and Phloem-Based Transport of CuO Nanoparticles in Maize (*Zea Mays L.*). *Environ. Sci. Technol.* **2012**, *46*, 4434–4441.
19. Priester, J. H.; Ge, Y.; Mielke, R. E.; Horst, A. M.; Moritz, S. C.; Espinosa, K.; Gelb, J.; Walker, S. L.; Nisbet, R. M.; An, Y.-J. Soybean Susceptibility to Manufactured Nanomaterials with Evidence for Food Quality and Soil Fertility Interruption. *Proc. Natl. Acad. Sci. U. S. A.* **2012**, *109*, E2451.
20. Musee, N. Nanotechnology Risk Assessment from a Waste Management Perspective: Are the Current Tools Adequate? *Hum. Exp. Toxicol.* **2011**, *30*, 820–835.

21. Park, B.; Donaldson, K.; Duffin, R.; Tran, L.; Kelly, F.; Mudway, I.; Morin, J. P.; Guest, R.; Jenkinson, P.; Samaras, Z.; et al. Hazard and Risk Assessment of a Nanoparticulate Cerium Oxide-Based Diesel Fuel Additive - a Case Study. *Inhalation Toxicol.* **2008**, *20*, 547–566.
22. Kiser, M. A.; Westerhoff, P.; Benn, T.; Wang, Y.; Perez-Rivera, J.; Hristovski, K. Titanium Nanomaterial Removal and Release from Wastewater Treatment Plants. *Environ. Sci. Technol.* **2009**, *43*, 6757–6763.
23. DuPont. Material Safety Data Sheet: Dupont Kocide 3000 Fungicide/Bactericide. http://www.solutionsstores.com/v/vspfiles/assets/images/kocide_3000_fungicide_msds.pdf (accessed 10/29/2015).
24. Daou, T. J.; Begin-Colin, S.; Grenèche, J. M.; Thomas, F.; Derory, A.; Bernhardt, P.; Legaré, P.; Pourroy, G. Phosphate Adsorption Properties of Magnetite-Based Nanoparticles. *Chem. Mater.* **2007**, *19*, 4494–4505.
25. Recillas, S.; Garcia, A.; Gonzalez, E.; Casals, E.; Puntes, V.; Sanchez, A.; Font, X. Preliminary Study of Phosphate Adsorption onto Cerium Oxide Nanoparticles for Use in Water Purification; Nanoparticles Synthesis and Characterization. *Water Sci. Technol.* **2012**, *66*, 503–509.
26. Bennett, S. W.; Keller, A. A. Comparative Photoactivity of CeO2, Gamma-Fe2O3, TiO2 and ZnO in Various Aqueous Systems. *Appl. Catal., B* **2011**, *102*, 600–607.
27. Collin, B.; Auffan, M.; Johnson, A. C.; Kaur, I.; Keller, A. A.; Lazareva, A.; Lead, J. R.; Ma, X. M.; Merrifield, R. C.; Svendsen, C.; et al. Environmental Release, Fate and Ecotoxicological Effects of Manufactured Ceria Nanomaterials. *Environ. Sci.: Nano* **2014**, *1*, 533–548.
28. Wang, J.; Yang, Y.; Zhu, H. G.; Braam, J.; Schnoor, J. L.; Alvarez, P. J. J. Uptake, Translocation, and Transformation of Quantum Dots with Cationic Versus Anionic Coatings by *Populus Deltoides X Nigra* Cuttings. *Environ. Sci. Technol.* **2014**, *48*, 6754–6762.
29. Zhu, Z. J.; Wang, H. H.; Yan, B.; Zheng, H.; Jiang, Y.; Miranda, O. R.; Rotello, V. M.; Xing, B. S.; Vachet, R. W. Effect of Surface Charge on the Uptake and Distribution of Gold Nanoparticles in Four Plant Species. *Environ. Sci. Technol.* **2012**, *46*, 12391–12398.
30. Conway, J. R.; Adeleye, A. S.; Gardea-Torresdey, J.; Keller, A. A. Aggregation, Dissolution, and Transformation of Copper Nanoparticles in Natural Waters. *Environ. Sci. Technol.* **2015**, *49*, 2749–2756.
31. Adeleye, A. S.; Conway, J. R.; Perez, T.; Rutten, P.; Keller, A. A. Influence of Extracellular Polymeric Substances on the Long-Term Fate, Dissolution, and Speciation of Copper-Based Nanoparticles. *Environ. Sci. Technol.* **2014**, *48*, 12561–12568.
32. Brady, N. C.; Weil, R. R. *Elements of the Nature and Properties of Soils*, 2nd ed.; Pearson Education: Upper Saddle River, NJ, 2003.
33. Raven, P. H.; Evert, R. F.; Eichhorn, S. E. *Biology of Plants*, 7th ed.; W. H. Freeman and Company: New York, NY, 2005.
34. Kupper, H.; Setlik, I.; Spiller, M.; Kupper, F. C.; Prasil, O. Heavy Metal-Induced Inhibition of Photosynthesis: Targets of *in vivo* Heavy Metal Chlorophyll Formation. *J. Phycol.* **2002**, *38*, 429–441.
35. Lv, J. T.; Zhang, S. Z.; Luo, L.; Zhang, J.; Yang, K.; Christie, P. Accumulation, Speciation and Uptake Pathway of ZnO Nanoparticles in Maize. *Environ. Sci.: Nano* **2015**, *2*, 68–77.
36. Almeelbi, T.; Bezbaruah, A. Nanoparticle-Sorbed Phosphate: Iron and Phosphate Bioavailability Studies with Spinacia Oleracea and Selenastrum Capricornutum. *ACS Sustainable Chem. Eng.* **2014**, *2*, 1625–1632.
37. Rui, Y.; Zhang, P.; Zhang, Y.; Ma, Y.; He, X.; Gui, X.; Li, Y.; Zhang, J.; Zheng, L.; Chu, S.; et al. Transformation of Ceria Nanoparticles in Cucumber Plants Is Influenced by Phosphate. *Environ. Pollut.* **2015**, *198*, 8–14.
38. Baker, N. R. Chlorophyll Fluorescence: A Probe of Photosynthesis *in vivo*. *Annu. Rev. Plant Biol.* **2008**, *59*, 89–113.
39. Barhoumi, L.; Oukarroum, A.; Taher, L. B.; Smiri, L. S.; Abdelmelek, H.; Dewez, D. Effects of Superparamagnetic Iron Oxide Nanoparticles on Photosynthesis and Growth of the Aquatic Plant Lemna Gibba. *Arch. Environ. Contam. Toxicol.* **2015**, *68*, 510–20.
40. Hasanuzzaman, M.; Hossain, M. A.; da Silva, J. A. T.; Fujita, M. *Plant Response and Tolerance to Abiotic Oxidative Stress: Antioxidant Defense Is a Key Factor* **2012**, 261–315.
41. Whiteside, M. D.; Treseder, K. K.; Atsatt, P. R. The Brighter Side of Soils: Quantum Dots Track Organic Nitrogen through Fungi and Plants. *Ecology* **2009**, *90*, 100–108.
42. Lopez-Moreno, M. L.; de la Rosa, G.; Hernandez-Viezcas, J. A.; Peralta-Videa, J. R.; Gardea-Torresdey, J. L. X-Ray Absorption Spectroscopy (XAS) Corroboration of the Uptake and Storage of CeO2 Nanoparticles and Assessment of Their Differential Toxicity in Four Edible Plant Species. *J. Agric. Food Chem.* **2010**, *58*, 3689–3693.
43. Xiong, Z. T.; Liu, C.; Geng, B. Phytotoxic Effects of Copper on Nitrogen Metabolism and Plant Growth in Brassica Pekinensis Rupr. *Ecotoxicol. Environ. Saf.* **2006**, *64*, 273–280.
44. Peng, H. Y.; Kroneck, P. M. H.; Kupper, H. Toxicity and Deficiency of Copper in Elsholtzia Splendens Affect Photosynthesis Biophysics, Pigments and Metal Accumulation. *Environ. Sci. Technol.* **2013**, *47*, 6120–6128.
45. Janik, E.; Maksymiec, W.; Gruszecki, W. I. The Photoprotective Mechanisms in Secale Cereale Leaves under Cu and High Light Stress Condition. *J. Photochem. Photobiol., B* **2010**, *101*, 47–52.
46. Werdan, K.; Heldt, H. W.; Milovancev, M. Role of pH in Regulation of Carbon Fixation in Chloroplast Stroma - Studies on CO2 Fixation in Light and Dark. *Biochim. Biophys. Acta, Bioenerg.* **1975**, *396*, 276–292.
47. Heldt, H. W.; Werdan, K.; Milovanc, M.; Geller, G. Alkalization of Chloroplast Stroma Caused by Light-Dependent Proton Flux into Thylakoid Space. *Biochim. Biophys. Acta, Bioenerg.* **1973**, *314*, 224–241.
48. Puig, S.; Andres-Colas, N.; Garcia-Molina, A.; Penarrubia, L. Copper and Iron Homeostasis in *Arabidopsis*: Responses to Metal Deficiencies, Interactions and Biotechnological Applications. *Plant, Cell Environ.* **2007**, *30*, 271–290.
49. Bouazizi, H.; Jouili, H.; Geitmann, A.; El Ferjani, E. Copper Toxicity in Expanding Leaves of Phaseolus Vulgaris L.: Antioxidant Enzyme Response and Nutrient Element Uptake. *Ecotoxicol. Environ. Saf.* **2010**, *73*, 1304–1308.
50. Alaoui-Sosse, B.; Genet, P.; Vinit-Dunand, F.; Toussaint, M. L.; Epron, D.; Badot, P. M. Effect of Copper on Growth in Cucumber Plants (Cucumis Sativus) and Its Relationships with Carbohydrate Accumulation and Changes in Ion Contents. *Plant Sci.* **2004**, *166*, 1213–1218.
51. Moore, R.; Clark, W. D.; Stern, K. R.; Vodopich, D. *Botany*; William C Brown Publishers: Dubuque, IA, 1995.
52. Du, W. C.; Sun, Y. Y.; Ji, R.; Zhu, J. G.; Wu, J. C.; Guo, H. Y. TiO2 and ZnO Nanoparticles Negatively Affect Wheat Growth and Soil Enzyme Activities in Agricultural Soil. *J. Environ. Monit.* **2011**, *13*, 822–828.
53. Zhao, L. J.; Hernandez-Viezcas, J. A.; Peralta-Videa, J. R.; Bandyopadhyay, S.; Peng, B.; Munoz, B.; Keller, A. A.; Gardea-Torresdey, J. L. ZnO Nanoparticle Fate in Soil and Zinc Bioaccumulation in Corn Plants (*Zea Mays*) Influenced by Alginate. *Environ. Sci.: Processes Impacts* **2013**, *15*, 260–266.
54. Morales, M. I.; Rico, C. M.; Hernandez-Viezcas, J. A.; Nunez, J. E.; Barrios, A. C.; Tafoya, A.; Pedro Flores-Marges, J.; Peralta-Videa, J. R.; Gardea-Torresdey, J. L. Toxicity Assessment of Cerium Oxide Nanoparticles in Cilantro (*Coriandrum Sativum L.*) Plants Grown in Organic Soil. *J. Agric. Food Chem.* **2013**, *61*, 6224–6230.
55. Judy, J. D.; Unrine, J. M.; Bertsch, P. M. Evidence for Biomagnification of Gold Nanoparticles within a Terrestrial Food Chain. *Environ. Sci. Technol.* **2011**, *45*, 776–781.
56. Keller, A. A.; Wang, H. T.; Zhou, D. X.; Lenihan, H. S.; Cherr, G.; Cardinale, B. J.; Miller, R.; Ji, Z. X. Stability and Aggregation of Metal Oxide Nanoparticles in Natural Aqueous Matrices. *Environ. Sci. Technol.* **2010**, *44*, 1962–1967.
57. Dudley, L. S.; Mazer, S. J.; Galusky, P. The Joint Evolution of Mating System, Floral Traits and Life History in *Clarkia* (Onagraceae): Genetic Constraints *Vs*. Independent Evolution. *J. Evol. Biol.* **2007**, *20*, 2200–2218.

58. Dudley, L. S.; Hove, A. A.; Mazer, S. J. Physiological Performance and Mating System in *Clarkia* (Onagraceae): Does Phenotypic Selection Predict Divergence between Sister Species? *Am. J. Bot.* **2012**, *99*, 488–507.
59. Kramer, D. M.; Johnson, G.; Kiirats, O.; Edwards, G. E. New Fluorescence Parameters for the Determination of Q(a) Redox State and Excitation Energy Fluxes. *Photosynth. Res.* **2004**, *79*, 209–218.
60. Cornelis, G.; Ryan, B.; McLaughlin, M. J.; Kirby, J. K.; Beak, D.; Chittleborough, D. Solubility and Batch Retention of CeO2 Nanoparticles in Soils. *Environ. Sci. Technol.* **2011**, *45*, 2777–2782.
61. Lopez-Moreno, M. L.; de la Rosa, G.; Hernandez-Viezcas, J. A.; Castillo-Michel, H.; Botez, C. E.; Peralta-Videa, J. R.; Gardea-Torresdey, J. L. Evidence of the Differential Biotransformation and Genotoxicity of ZnO and CeO2 Nanoparticles on Soybean (*Glycine Max*) Plants. *Environ. Sci. Technol.* **2010**, *44*, 7315–7320.